3D COMBINED FRACTAL DIPOLE WIRE ANTENNA

Assist. Prof. Refa'at Talib Hussein

Receipted: 22 /1 /2007
Accepted: 14 /11/2007

Abstract

This work presents a numerical study for a new design of small size and multi-band fractal dipole antennas which is constructed by combining two fractal geometries to get the main antenna body. In this work a 3D combined fractal dipole antenna will be designed based on Hilbert and Koch curves to form the antenna geometry by using method of moment technique. Numerical simulations presented here also indicate that antenna size can be further reduced by 3D combined.

KEY WORDS
Fractal antennas, 3D combined fractal antennas, Multi-band antennas.

الخلاصة

تم في هذا البحث استعراض دراسة عددية للنوع المقترح من الهوائيات الجزئية ثنائية القطب ذات الحجم الصغير و الترددات المتعددة. تم بناء التركيب المقترح من الهوائيات على أساس فكرة دمج نوعين مختلفين من الهوائيات الجزئية المألوفة. تم تصميم الهوائي ثنائي القطب الجديد الثلاثي الأبعاد على أساس دمج منحني هلبرت و منحني كوخ لتكوين هذا الهوائي.
تم أجراء المحاكاة العددية باستخدام تقنية طريقه العزوم و تم استعراض النتائج التي تشير إلى إن حجم الهوائي يمكن تقليله بصوره أكثر باستخدام هذا النوع من الهوائيات.

Electrical and Electronic Engineering Department University of Technology Baghdad-IRAQ
Email: zubidaflower@yahoo.com

1. Introduction

Fractals were first defined by Mandelbrot in 1975[1] as a way of classifying structures whose dimensions where not whole numbers and to describe a family of complex shapes that possess inherent self-similarity or self-affinity in their geometrical structure [2]. These geometries have been used previously to characterize unique occurrence in nature that where difficult to define with Euclidean geometries, including the length of coastline, density of clouds, and the branching of trees [2]. The fractal antenna is one of their applications. Puente. C, *et al.*,[3] in 2000 investigated the properties of Koch curve fractal monopole antenna, as shown in figure (1). Vinoy K.J, *et al.* [4] in 2001 investigated the usefulness of fractal Hilbert curves in antenna geometry, as shown in figure (2). This curves meandered in a specific way to fill the nearby space. The properties of the fractal antennas are exploited in realizing a 'small' resonant antenna. This approach has resulted in an antenna size smaller than λ/10 and still resonant, with performance comparable to a dipole whose resonant length close to λ/2. Numerical predictions of the input impedance of the antenna have been compared with experiments in [4].

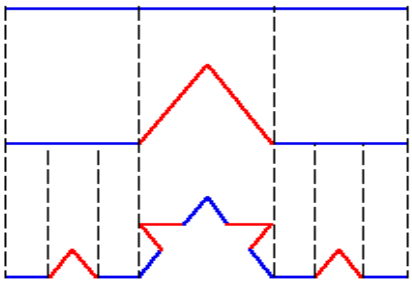

Figure 1. Monopole Koch curve (0, 1st, and 2nd Iteration).

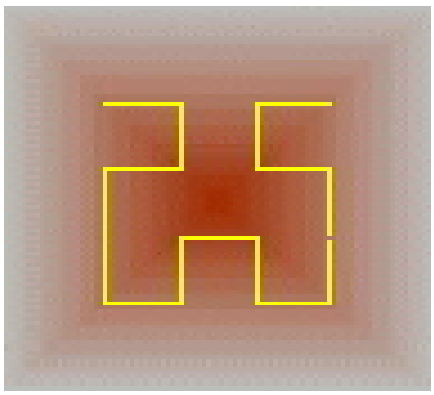

Figure 2. 2nd iteration Hilbert curve.

The main advantage of using Hilbert geometry in the design of antennas is the reduction in the overall size of the resonant antenna. More size reduction can be obtained by superimposing Koch curves on to construct the 3D-combined fractal antenna. It is obvious that this approach would increase the overall curve-length and gives the resulted antenna properties that related to the basic geometries that constructed this combined fractal antenna.

2. 3D-Combined Antenna Description

In the previous section the properties of antennas using a single fractal geometry was investigated by many authors [3-6], but all these antennas were depending on a single fractal geometry as the antenna body and the resulted antenna had a properties related to this single geometry. While, 2D-combined fractal geometry was investigated by some authors [7, 8].

In this paper a proposed type for fractal antenna design will be numerically simulated. This proposed way including to construct 3D-antenna fractal geometry by combining two fractal geometries. The proposed antenna is consist of the 1st iteration Koch curve basic geometry, as shown in figure (3), replaced with the segment lines of the 2nd iteration Hilbert curve fractal geometry in figure (2) and in the planes perpendicular to the plane of the Hilbert plane as shown in figure (4). Also, the proposed fractal antenna design type will be numerically simulated based on Method of Moment (MoM) [9].

The polar plots of normalized electric field patterns in the three orthogonal planes (xy-plane, xz-plane and yx-plane) at each resonant frequency in table (1) of this combined geometry are shown in figures (5-8) where the feeding point of the combined geometry placed in the xy-plane.

4. Conclusion

The simulation of fractal antennas shows that these antennas have their first resonance frequency below the design frequency [3-6], but with this 3D-combine antenna the first resonance frequency was very near to the design frequency. The difference in this case between the design frequency and the first resonance frequency equal to 32MHz, and this mean the two frequencies are very close to each other more than if we used a single geometry in the antenna design.

In the design of Hilbert curve and Koch curve dipoles the number of resonant frequencies was proportional to the number of iteration order of the geometry. Therefore a Hilbert curve with 2^{nd} iteration geometry have a two resonance frequencies, and 1^{st} iteration Koch curve geometry have one resonance frequency, but with 3D-combine geometry four resonant frequencies appeared by combined 2^{nd} order and 1^{st} order geometries.

This 3D geometry has a high degree of similarity between the radiation of the electric field patterns at different resonance frequencies compared with 2D-combined fractal geometry [7, 8]. Also, the field patterns of the 3D proposed model have a similar behaviour, such as a linear polarization in the planes xz and xy and an elliptical polarization in the plan yz. The input impedance of this combine antenna at the upper three resonance frequencies is around 100 Ω, as shown in table (1).

Reference

[1] Facon, K.," Fractal Geometry: Geometry mathematical foundation and application", England, John Wiley, 1990.

[2] Werner, D., Ganguly S., "An overview of Fractal Antennas Engineering Research", IEEE Antenna & Propagation Magazine, vol. 45, no. 1, pp. 38-56, 2003.

[3] Puente, C., et al, "The Koch monopole a small fractal antenna", IEEE Transaction on antennas and propagation, vol. 48, pp. 1773-1781, 2000.

[4] Vinoy, K.J., Jose K.A., Varadan V.K., and Varadan V.V., "Hilbert curve fractal antenna: a small resonant antenna for VHF/UHF applications, Microwave & Optical Technology Letters, vol. 29, pp.215-219, 2001.

[5] Vinoy, K.J., Jose A., Vijay K., "On the Relation ship Between Fractal Dimension and the Performance of Multi-Resolution Dipole Antennas Using Koch Curves", IEEE Transactions on Antennas and Propagation, vol. 51, no. 9, Sept. 2003.

[6] Vinoy, K.J., Jose K.A., Varadan V.K., and Varadan V.V., "Resonant Frequency of Hilbert Curve Fractal Antennas", IEEE AP-S International Symposium, Boston, July 8-13, 2001 Digest vol.3, pp. 648-651, 2001.

[7] Vinoy, K.J., "Fractal Shaped Antenna Elements for Wide- and Multi- band Wireless Applications", A Thesis in Eng. Science and Mechanics, The Pennsylvania State University 2002.

[8] Tahir, M. K., "Analysis, Design and Simulation of combined Fractal Dipole Antennas", M.Sc. Thesis, University of Technology, Dec. 2005.

[9] Stutzman W., and G.A. Thiele, "Antenna Theory and Design", New York: John Wiley, 2^{nd}, 1998.

[10] NEC-2 manuals: www.nec2.org

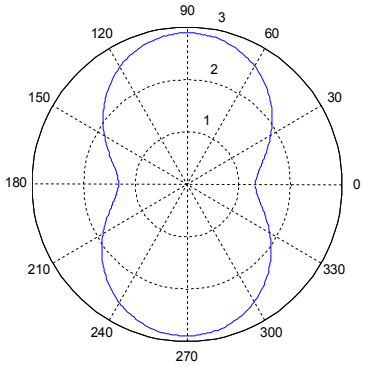

(a) E_{φ} at xy-plane

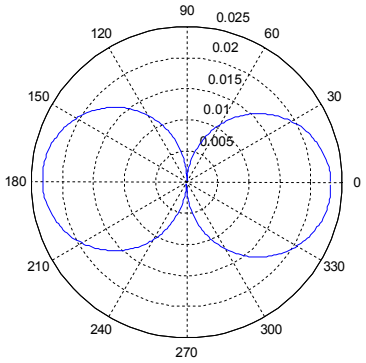

(d) E_{θ} at xz-plane

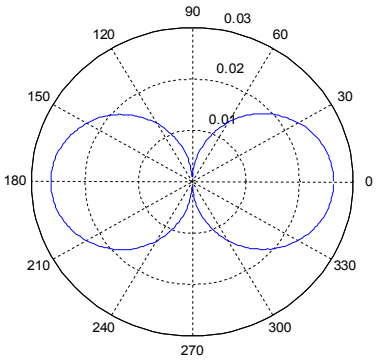

(b) E_{θ} at xy-plane

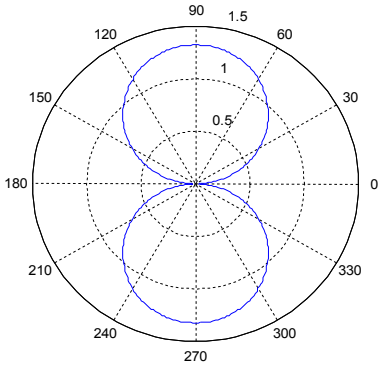

(e) E_{φ} at yz-plane

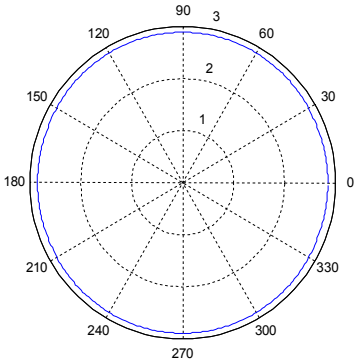

(c) E_{φ} at xz-plane

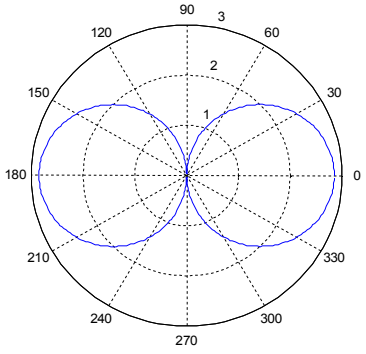

(f) E_{θ} at yz-plane

Figure 5. Normalized electric field

patterns for f = 468MHz.

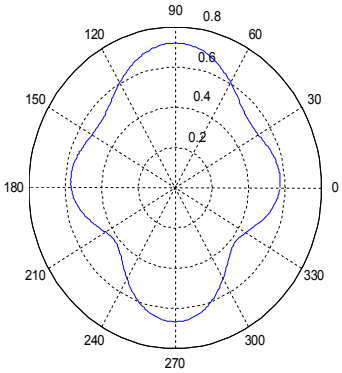

(a) E_φ at xy-plane

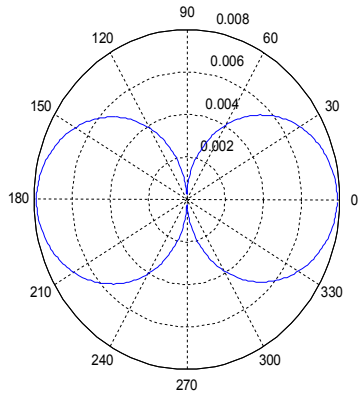

(d) E_θ at xz-plane

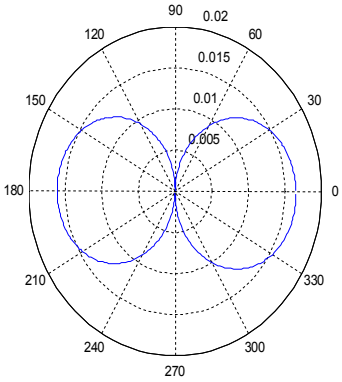

(b) E_θ at xy-plane

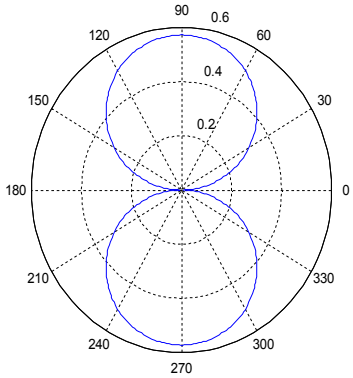

(e) E_φ at yz-plane

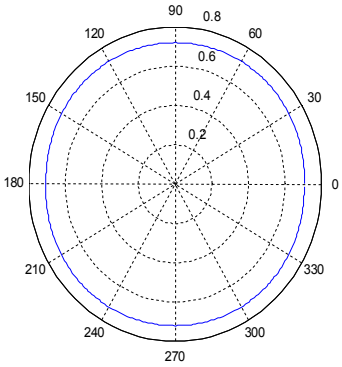

(c) E_φ at xz-plane

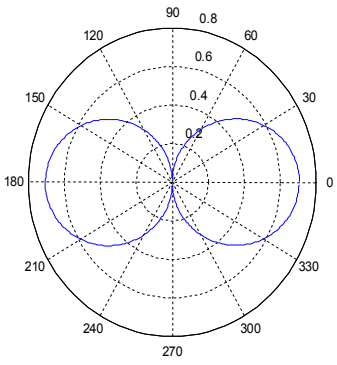

(f) E_θ at yz-plane

Figure 6. Normalized electric field

patterns for f = 1319MHz

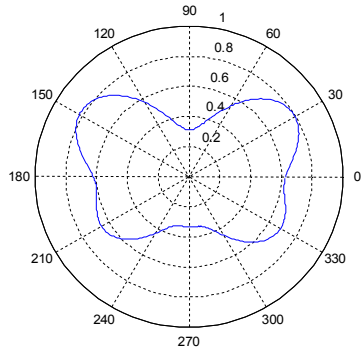

(a) E_φ at xy-plane

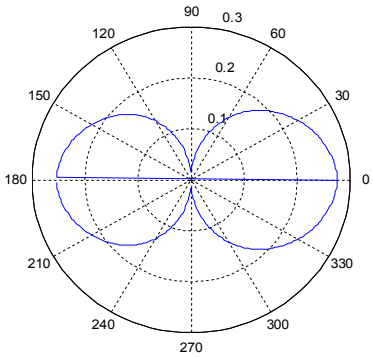

(d) E_θ at xz-plane

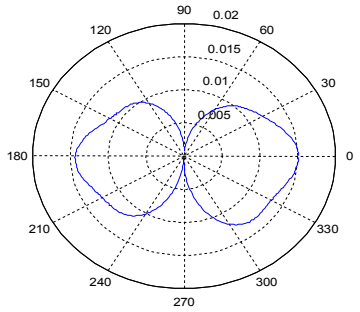

(b) E_θ at xy-plane

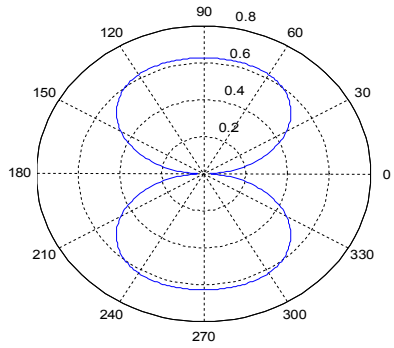

(e) E_φ at yz-plane

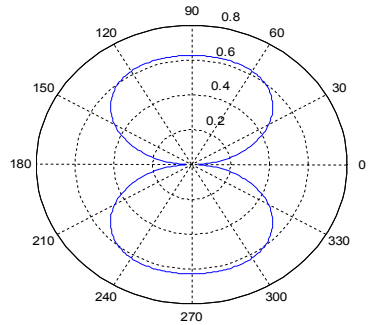

(c) E_φ at xz-plane

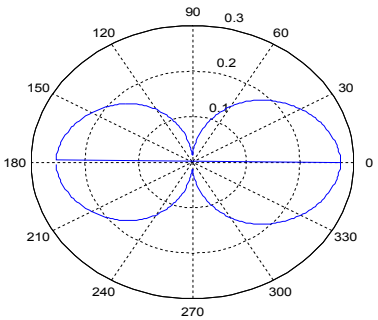

(f) E_θ at yz-plane

Figure 7. Normalized electric field patterns for f = 2086MHz.

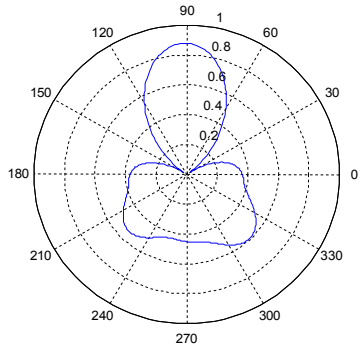

(a) E_φ at xy-plane

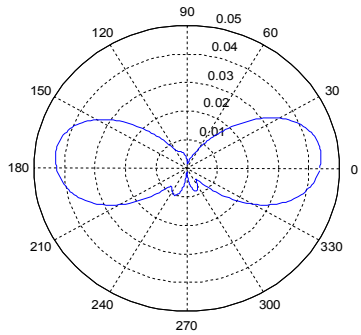

(b) E_θ at xy-plane

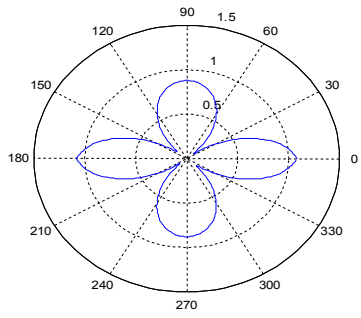

(c) E_φ at xz-plane

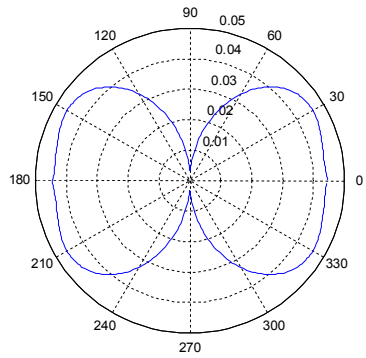

(d) E_θ at xz-plane

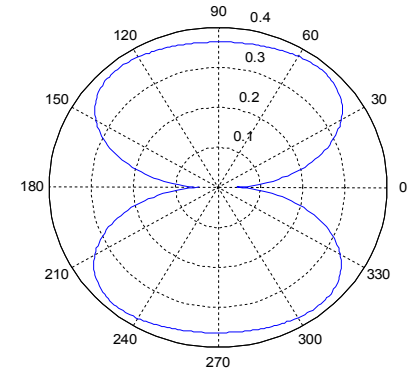

(e) E_φ at yz-plane

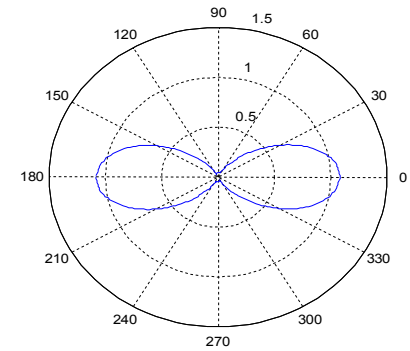

(f) E_θ at yz-plane

Figure 8. Normalized electric field patterns for f = 2892MHz.